Published OnlineFirst December 10, 2020; DOI: 10.1158/1541-7786.MCR-20-0482

N-Acetyl-L-cysteine Promotes *Ex Vivo* Growth and Expansion of Single Circulating Tumor Cells by Mitigating Cellular Stress Responses

Teng Teng[1,2,3], Mohamed Kamal[1,2,4], Oihana Iriondo[1,2], Yonatan Amzaleg[1,2,5], Chunqiao Luo[6], Amal Thomas[7], Grace Lee[1,2], Ching-Ju Hsu[8], John D. Nguyen[1,2], Irene Kang[2], James Hicks[8], Andrew Smith[7], Richard Sposto[6], and Min Yu[1,2]

ABSTRACT

Circulating tumor cells (CTC) can be isolated via a minimally invasive blood draw and are considered a "liquid biopsy" of their originating solid tumors. CTCs contain a small subset of metastatic precursors that can form metastases in secondary organs and provide a resource to identify mechanisms underlying metastasis-initiating properties. Despite technological advancements that allow for highly sensitive approaches of detection and isolation, CTCs are very rare and often present as single cells, posing an extreme challenge for *ex vivo* expansion after isolation. Here, using previously established patient-derived CTC lines, we performed a small-molecule drug screen to identify compounds that can improve *ex vivo* culture efficiency for single CTCs. We found that N-acetyl-L-cysteine (NAC) and other antioxidants can promote *ex vivo* expansion of single CTCs, by reducing oxidative and other stress particularly at the initial stage of single-cell expansion. RNA-seq analysis of growing clones and nongrowing clones confirmed the effect by NAC, but also indicates that NAC-induced decrease in oxidative stress is insufficient for promoting proliferation of a subset of cells with predominant senescent features. Despite the challenge in expanding all CTCs, NAC treatment led to establishment of single CTC clones that have similar tumorigenic features.

Implications: Through a small molecule screen and validation study, we found that NAC could improve the success of *ex vivo* expansion of single CTCs by mitigating the initial stress, with the potential to facilitate the investigation of functional heterogeneity in CTCs.

Introduction

Circulating tumor cells (CTC) are cancer cells shed from primary or metastatic lesions into systemic circulation. Because CTCs can be shed from multiple active tumor lesions, and they contain precursors that can eventually initiate metastasis, CTCs are considered a liquid biopsy for solid tumors (1, 2). It has been shown that high numbers of CTCs correlate with a worse prognosis in several types of cancer (1, 3). Despite significant variability between patients and disease stages, CTCs are generally very rare. Most patients with metastatic cancers, including prostate, ovarian, breast, gastric, colorectal, bladder, renal, non–small cell lung, and pancreatic cancers, have low numbers of CTCs in a tube of blood, according to an analysis using the CellSearch platform, which captures CTCs based on EpCAM expression (4). Although technologies that do not solely rely on EpCAM-surface expression have been reported to capture a higher number of CTCs (1, 5, 6), the quantity remains too low for downstream functional analysis in most cases.

Several studies have shown successful *ex vivo* expansion of CTCs isolated from patients with breast (7), colorectal (8), and prostate (9) cancer. These CTC lines have provided sufficient amounts of material for many analyses, including xenograft analysis and drug susceptibility assessment (7, 10). However, the efficiency of establishing the *ex vivo* culture of CTCs is extremely low, limiting its broad application to the majority of the patients with cancer (10). This low efficiency may be due to limited quantities, low capture efficiency, the harshness of the procedure, and the vulnerability of CTCs in circulation. Therefore, improved culture conditions for expanding CTCs may help resolve their molecular and phenotypic properties.

Because of the rarity of CTCs, optimizing culture conditions has been challenging. We previously reported *ex vivo* culture of CTCs derived from patients with metastatic breast cancer and established several CTC lines (7). These CTC lines exhibit metastatic potential that represents the major metastatic lesions in corresponding patients (11). However, like primary tumors, CTCs are heterogenous with different EMT and stem cell status (12–16). To functionally understand the intrapatient's heterogeneity of CTCs, it will be very useful to establish multiple CTC clones from individual patients. Although our CTC lines

[1]Department of Stem Cell Biology and Regenerative Medicine, Keck School of Medicine of the University of Southern California, Los Angeles, California. [2]USC Norris Comprehensive Cancer Center, Keck School of Medicine of the University of Southern California, Los Angeles, California. [3]The Second XiangYa Hospital of Central South University, XiangYa School of Medicine, Central South University, ChangSha, HuNan, China. [4]Department of Zoology, Faculty of Science, University of Benha, Benha, Egypt. [5]Center for Craniofacial Molecular Biology, Ostrow School of Dentistry of the University of Southern California, Los Angeles, California. [6]Biostatistics Core, Department of Preventive Medicine, Keck School of Medicine of the University of Southern California, Los Angeles, California. [7]Department of Molecular and Computational Biology, USC David and Dana Dornsife College of Letters, Arts and Sciences, University of Southern California, Los Angeles, California. [8]Bridge Institute, USC David and Dana Dornsife College of Letters, Arts and Sciences, University of Southern California, Los Angeles, California.

Note: Supplementary data for this article are available at Molecular Cancer Research Online (http://mcr.aacrjournals.org/).

T. Teng and M. Kamal contributed equally to this article.

Corresponding Author: Min Yu, University of Southern California, 1450 Biggy Street, NRT 3507, Los Angeles, CA 90033. Phone: 323-442-7943; E-mail: minyu@med.usc.edu

Mol Cancer Res 2021;19:441–50

doi: 10.1158/1541-7786.MCR-20-0482

Published OnlineFirst December 10, 2020; DOI: 10.1158/1541-7786.MCR-20-0482

can be maintained long term in culture (in suspension and physiologic oxygen level, mimicking the environment of CTCs in venous blood circulation), when dissociated and plated as single cells, it is extremely difficult for majority of these cells to expand successfully. This suggests that establishing single CTC lines from freshly isolated CTCs of patients with cancer will be even harder. Hence, we used single CTCs as a platform to screen a small molecule library to identify compounds that promote their expansion in culture.

Materials and Methods

Cell culture

CTC lines were previously derived from patients with metastatic breast cancer (7). CTC lines were authenticated by autosomal STR profiles by University of Arizona genetics core and were routinely tested for *Mycoplasma* every 2 to 3 months. Cells used for all experiments were within 24 months from thawing. CTC lines were cultured in ultralow attachment plates with RPMI1640 medium, supplemented with EGF (20 ng/mL), bFGF (20 ng/mL), 1× B27, and 1× antibiotic/antimycotic, in 4% O_2 and 5% CO_2. Single CTCs were cultured in GravityTRAP ULA 96 well Plates (InSphero). Wells on the edges of the plates were not used to avoid influence from evaporation. Media with fresh compounds were exchanged every 3 days by inserting pipet tips onto the platform of the wells to prevent accidentally aspirating suspended CTCs at the bottom. CTC numbers were counted manually under an inverted microscope every 6 days.

FACS

Cells were pelleted and resuspended into single-cell suspension in 1% BSA in PBS buffer with 7-AAD. Live single CTCs were sorted directly into 96-well GravityTRAP ULA Plates using aMoFlo cell sorter (Beckman Coulter). An inverted microscope was used to manually confirm that there was 1 CTC per well, 1 hour after sorting.

Compounds screening

Compounds were from the StemSelect library obtained from the Choi Family Therapeutic Screening Facility at the Eli and Edythe Broad CIRM Center for Regenerative Medicine and Stem Cell Research at USC. Each compound was given a code to ensure unbiased assessment and blinded to the investigators. Compound information is listed in Supplementary Table S1. In the first-round screening, compounds were used with 1 μmol/L concentration. Stocks of compounds (10 mmol/L concentration in DMSO) were stored in aliquots at −80°C. All compounds were thawed and refrozen for a maximum of 2 times. In the second-round validation, fresh compounds were dissolved in DMSO (Millipore sigma), and aliquots were stored at −20°C and used only once without refreezing. Only wells started from single cells on day 0 after sorting were used in the screening experiment. Data collection was done in batches.

Spike-in experiment

Healthy volunteers' blood samples were collected following protocols approved by the Institutional Review Board (IRB) at the University of Southern California. GFP-positive CTC lines (50 cells/mL) were spiked into the blood samples from healthy volunteers, and RosetteSep CTC Enrichment Cocktail Containing Anti-CD56 was used to enrich CTCs from spiked-in samples. Isolated CTCs were cultured in GravityTRAP ULA Plate 96 wells. Each patient CTC cell line was processed by 2 different researchers.

Single CTC clones

NAC clones were generated by treating single CTCs with 300 μmol/L NAC media for 24 days before switching to regular CTC media. Control single clone lines were established in the same batch using regular CTC media.

Xenograft assay and hematoxylin and eosin staining

The animal protocol was approved by the Institutional Animal Care and Use Committee of the University of Southern California. Six-week-old female NSG mice (The Jackson Laboratory) were anesthetized with isoflurane and 20,000 GFP/luc-positive single clone cells in 100 μL of 1:1 PBS and Corning Matrigel Matrix (phenol-red free) were injected into the fourth mammary fat pad. To evaluate the growth of primary tumors, mice were intraperitoneally injected with 150 μL of D-luciferin substrate at 30 mg/mL (Sid Labs) and imaged within 15 minutes. Signals from luciferase-tagged cells were monitored at day 0 after injection and weekly by *in vivo* imaging using IVIS Lumina II (PerkinElmer) for 5 weeks. Mice were sacrificed after 8 weeks, and their organs were dissected and imaged. Primary tumors were collected and fixed with 10% formalin overnight and sectioned for 5 μm thickness. H&E staining was performed using Varistain Gemini ES Automated Slide Stainer in USC's Histology Laboratory (HIST). Images were taken with a 20× objective in Keyence (BZ-II Analyser, Keyence).

Patient samples

Ten milliliters of blood was collected from each of a total of 12 patients with breast cancer (stage IV) at either the USC Norris Comprehensive Cancer Center or Los Angeles-County + University of Southern California (USC) Medical Center. All experiments were performed following the ethical principles embodied in The Belmont Report, under protocol No. 1B-11–1 approved by the IRB at USC. Informed consents were signed by all patients and/or their legal guardian/s.

Isolation of single CTCs

Single CTCs were detected and retrieved using the negative selection protocol of PIC&RUN assay as previously described (17). Briefly, 7.5 mL of blood was added to each AccuCyte Separation Tube (RareCyte) and tubes were centrifuged twice in a special device to collect buffy coats in 1 mL of CTC media. Buffy coats were stained with a cocktail of immune cell markers (IM) antibodies (CD45, CD14, and CD16) and Cell-Tracker green for 30 min at 37°C. Stained buffy coats were seeded on polyhema coated cyteslides and scanned semiautomatically using RareCyte fluorescence. When a CTC was detected, the Rarecyte ceramic tip needle was operated semiautomatically to pick up the cell of interest in a draw volume of 50 nL to 0.5 μL, and deposit it in a PCR tube contains 50 μL of media. PCR tubes were pulse spun, their contents were moved to a well of a 96-well GravityTRAP ultralow plate (InSphero) and plates were incubated at 37°C, 5% CO_2 and 4% O_2 for 3 weeks. Media was replaced every 3 to 4 days and cells were checked every week.

Copy number variation analyses

Single-cell genomic copy number profiling was carried out essentially as previously described (18) with exceptions as noted. After lysis of individual cells in 1.5 μL lysis buffer (1:1 solution of 100 mmol/L DTT + 400 mmol/L KOH) for 2 minutes at 95°C, DNA was amplified using the WGA4 Genomeplex Single Cell Whole Genome Amplification Kit (Sigma-Aldrich, cat#. WGA4) for 23 cycles. Amplified DNA was purified using a QIAquick PCR Purification Kit (Thermo Fisher

Published OnlineFirst December 10, 2020; DOI: 10.1158/1541-7786.MCR-20-0482

Scientific, cat#. K210012). DNA was eluted in 60 μL of TE-buffer and quantified by Qubit. Indexed Illumina sequencing libraries were constructed and barcoded using the NEBNext Ultra DNA Library Preparation Kit for Illumina (New England Biolabs, cat#. E7370L). Amplified DNA fragments with target size were selected using Agencourt AMPure XP beads (Beckman Coulter, cat#. A63880) and further confirmed by Bioanalyzer High Sensitivity DNA Analysis (Agilent, cat# 5067–4626). Libraries were sequenced using the Illumina NextSeq 500 at Fulgent Biosciences. 30 bp were trimmed off the 5' end of each read to remove the WGA4 adapter sequence before alignment to the hg19 reference genome using the Bowtie algorithm. The resulting BAM file was sorted and PCR duplicates were removed using SAMtools. Copy number profiles were obtained by sorting reads into 5,000 informatically derived "bins" across the genome with sizes normalized to contain equal lengths of uniquely mapping sequence (approximately 0.5 Mbp) according to the UCSC reference genome Hp37 (19). Finally, an R script utilizing the Bioconductor package, DNAcopy_1.26.0 (http://bioconductor.org/packages/DNAcopy/), was used to normalize and segment the bin counts across each chromosome generating a genome-wide CNA profile with a resolution of approximately 1.5 Mbp (19).

RNA sequencing analysis

BRx68-GFP$^+$ cells were sorted, with 1 cell per well, using the MoFlo cell sorter (Beckman Coulter). Single cells were cultured in the presence of CTC media containing either 1 μmol/L of P1C2, P4D8, or P1G7, or 300 μmol/L of NAC or a combination of 1 μmol/L of P1C2 and 300 μmol/L of NAC. Cells cultured in media containing DMSO served as a control. All cells were cultured for either 6 days or 13 days at 37°C, 5% CO_2 and 4% O_2, and media was changed every 3 days. For both day 6 and day 13 groups, clones with more than 3 cells at day 6 were harvested and pooled to a maximum of 50 cells as growing clones, and those that never divided were collected as nongrowing clones. Pooled samples were processed using SMARTer chemistry (SMART Seq v4 Ultra Low Input RNA Kit for Sequencing, Takara Clontech), according to manufacturer's instructions to generate cDNA libraries for mRNA sequencing. All cDNA samples were run on a TapeStation system (High Sensitivity D5000 DNA Analysis Kit as per manufacturer's protocol). cDNA libraries were prepared using the Nextera XT DNA Library Prep Kit (Illumina) with Nextera index kit index 1 (i7) and index 2 (i5) adapters. Libraries were sequenced on an Illumina NextSeq500 to obtain 75 bp-long single-end reads.

RNA sequencing (RNA-seq) reads were trimmed for Illumina adapter sequences using Trim Galore under default parameters. Trimmed reads were then mapped to the human genome build GRCh37 from Ensembl (http://ftp.ensembl.org/pub/current_fasta/homo_sapiens/dna/) using STAR under optimized parameters for single-end sequenced data. Aligned reads were then counted via featureCounts and piped into DESeq2 for normalization to sequencing depth and downstream analysis. For purposes of producing the PCA plot, count data was transformed via the vst function to eliminate the experiment-wide trend of variance over mean and the plot was produced using ggplot2. For the PCA plot, batch effects were corrected using the function removeBatchEffect from limma. Differential expression analysis was performed controlling for batch effects. The contrast function was used to compare all conditions at day 13 versus day 6, and each treatment versus control at each time point, or growing NAC-treated versus non growing at day13. To detect enriched pathways within differentially expressed genes (DEGs), genes with a FDR of 0.05 and $\log_2$ fold change of >1.5 were piped into IPA and GO analysis. DEGs with fold change ≥ 2 and FDR ≤ 0.05 identified from a previously published study (20) are used as marker genes for quiescence and senescence states. Heatmap based on the normalized expression values of the senescent and quiescent marker genes is generated using ComplexHeatmap package (21). The GO enrichment analysis is performed using the Bioconductor package GOseq (22).

Statistical analysis

For the screening analysis, the number of cells grown over time per well per plate per batch was represented as either area under curve (AUC) or absolute number of cells. AUC was calculated for each well in each batch, by plotting days in the *x*-axis and the corresponding number of cells in the *y*-axis, then drawing a line to connect the number of cells from the starting count day to the next count day until the end day, and finally calculating the area under this line as the sum of areas of trapezoids. If there are two count days, there will be one trapezoid; if there are three count days, there will be two trapezoids, and so on. For each trapezoid, area = 1/2*length of day interval* (number of cells in day x1 + number of cells in day x2). A Wilcoxon rank sum test was performed to compare AUC of each drug to AUC of CT (control with CTC media only) or CD (control with matching amount of DMSO in CTC media) within each batch. *P* values were adjusted by Benjamini–Hochberg Procedure to control the FDR. In the validation experiments, drugs with adjusted P values ≤ 0.2 were considered as statistically different from CT/CD. Statistical tests were performed using R. For absolute number of cells quantification, total number of cells at end of experiment in each well in each batch was compared between treated cells and untreated control and significance was analyzed with Student *t* test. For other experiments, data were analyzed with Student *t* test, and represent the means ± SEM of at least triplicate samples or averages ± SD of independent analyses, as indicated. $P < 0.05$ was considered statistically significant. Statistical tests were performed with GraphPad Prism7 statistical software.

Glutathione measurement

A total of 1×10^6 BRx68 cells were cultured with or without 300 μmol/L NAC for 6 or 13 days. At the end of incubation periods, cells were washed in ice cold PBS, lysed in 5% 5-sulfo-salicylic acid dehydrate by vortexing and repeating cycles of freeze-thaw, then centrifuged at 14,000 rpm for 10 minutes and supernatant was transferred to clean tubes. Glutathione (GSH) was measured using a GSH Colorimetric Detection Kit (Invitrogen) following the manufacturer's instructions.

Data and materials availability

All data needed to evaluate the conclusions in the article are present in the article and/or the Supplementary Materials. RNA-seq data are deposited at GEO database (GSE134138). Additional data related to this article may be requested from the authors.

Results

Initial low-confidence screening for single CTC expansion

We first performed a low-confidence initial screen using single CTCs sorted from our CTC lines with 317 compounds from the StemSelect library (Supplementary Table S1) as described in the methods and shown in **Fig. 1**. This initial screen was performed with 12 to 18 wells per compound, totaling 28 successful batches with 235 plates from 3 patient-derived CTC lines (BRx68, BRx07,

Published OnlineFirst December 10, 2020; DOI: 10.1158/1541-7786.MCR-20-0482

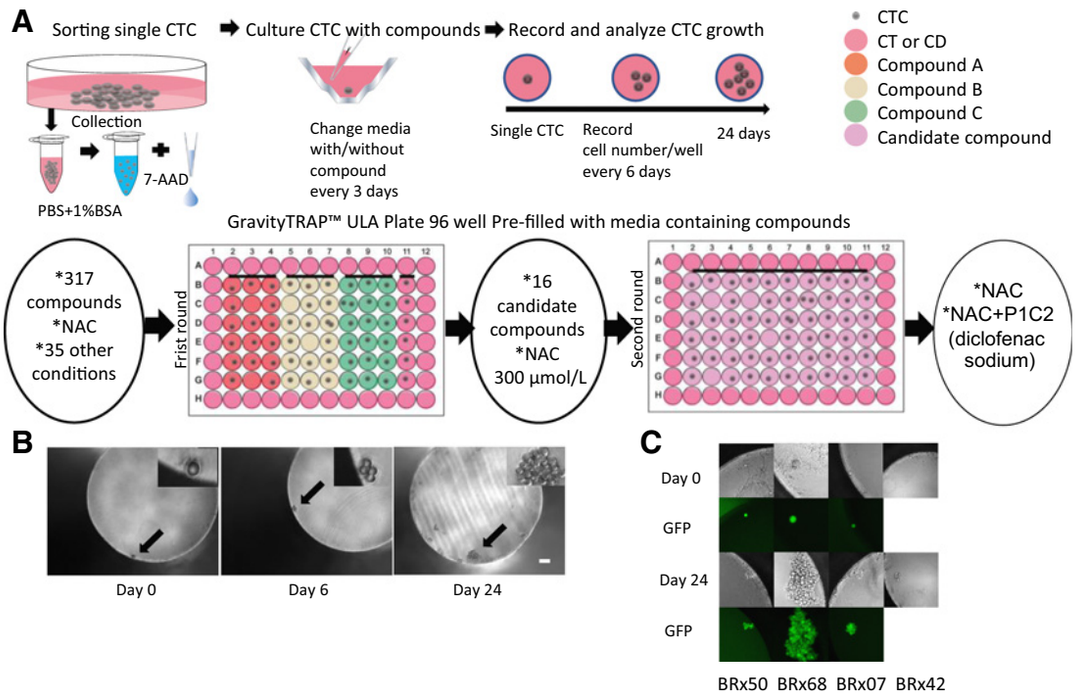

Figure 1.

Illustration of the single-cell drug screen process. **A,** Illustration of the small-molecule screening process (top) and the summary of results from the first and second round screenings (bottom). **B,** Representative phase-contrast images of the growth of a single BRx68 CTC at different time points. Scale bar, 200 µm. **C,** Representative phase-contrast and GFP-fluorescent images of CTC clones generated from different CTC lines (BRx50, BRx68, BRx07, and BRx42). BRx42 cells used are not GFP-transduced.

and BRx50). DMSO controls were included in each batch and the compounds were tested blindly with code names. Because of significant heterogeneity in single cells, the limited number of wells tested for each compound in this initial screen is not sufficient for statistical analysis. Therefore, to identify a recurring pattern of compounds that function in similar pathways, we analyzed all the compounds that showed a higher median value of growth. To capture the effect over several time points for multiple wells, we used AUC calculation of cell numbers over time (Supplementary Fig. S1), compared with controls in the same batch, including CTC media only (CT) or media with vehicle DMSO (CD). Among the 130 compounds detected to have a higher median AUC than the controls (**Table 1**, Supplementary Tables S2 and S3), we found many compounds with similar biological functions. Seven of 12 cyclooxygenase (COX) inhibitors, 6 of 11 antioxidants and free radical scavengers, and 4 of 4 5′ adenosine monophosphate-activated protein kinase (AMPK) activators increased CTC growth in this initial screen (**Table 1**). Because all 3 pathways have been previously linked with reducing cellular ROS levels (23–25) and given recent reports showing the role of antioxidants in CTC survival, we also tested a commonly used antioxidant N-Acetyl-L-cysteine (NAC). We first evaluated the effect of several different concentrations of NAC on the BRx68 line in two different batches and found the 200 and 300 µmol/L NAC showed the most significant effect in promoting single CTC proliferation (Supplementary Fig. S2A and S2B). Therefore, we selected NAC and several different compounds from these pathways to further validate in a second-round test using a larger number of wells for statistical evaluation.

Validation of candidate compounds

We selected 16 compounds plus NAC from the most promising biological activity categories to validate in 4 patient-derived CTC lines (BRx07, BRx42, BRx50, and BRx68), using 36 different concentrations or combinations. This totaled 13 batches consisting 166 plates with 60 wells per plate.

Results showed that the best compounds that are universal to all 4 CTC lines are NAC at 300 µmol/L, or NAC (300 µmol/L) in combination with the P1C2 compound—a COX-1/2 inhibitor, Diclofenac Sodium (1 µmol/L or 0.5 µmol/L; Supplementary Tables S4 and S5). Compared with controls, NAC or NAC+P1C2 consistently showed statistically significant improvement for single CTC expansion across many different batches for all 4 CTC lines (**Fig. 2A** and **B**; Supplementary Fig. S2C). For BRx50 and BRx42 lines, which are extremely difficult to expand as single cells, the addition of these compounds can lead to the successful generation of single cell clones. A few other compounds were also confirmed to increase CTC expansion but in a cell line–specific manner (Supplementary Fig. S2D–S2F; Supplementary Table S4). Therefore, we decided to focus on NAC.

To mimic the CTC isolation procedure, we performed spiked-in experiments with 3 CTC lines (BRx42, BRx50, and BRx68) into healthy donors' blood. We used the RosettSep CTC isolation method to isolate the spiked CTCs and separated isolated CTCs equally into wells with control media or with NAC or NAC plus P1C2. Compared with the control condition, NAC or NAC plus P1C2 significantly increased the growth of isolated CTCs (Supplementary Fig. S3). This confirmed the effects of these compounds on expanding CTCs that have been processed through an isolation procedure.

Published OnlineFirst December 10, 2020; DOI: 10.1158/1541-7786.MCR-20-0482

Table 1. Analysis of a list of identified compounds from the initial screen.

Biological activity	Number of compounds with AUC > controls	Number of compounds tested	Compounds chosen for validation
COX Inhibitor	7	12	P1G7; P1C2; P3B5; P2D9
Histone deacetylase inhibitors	8	15	P1G3[a]
Sonic Hedgehog signaling antagonists/inhibitors	7	10	P2F10
Antioxidants and free radical scavengers	6	11	P1C6; P1F4; P4D8
Tyrosine kinase inhibitors/c-kit	5	6	P2H7
SIRT Inhibitor	5	7	P1G3
PARP Inhibitor	4	7	P4E9
Wnt Antagonist/activates	4	8	P1B6
STAT Signaling inhibitors/enhancer	4	7	P1G11
Ca2+ channel	4	20	
AMPK activator	4	4	P1A7; P2C2
Proteasome-ubiquitination inhibitors	3	6	P1H5
Phosphodiesterase inhibitors	3	6	
Phosphatase inhibitors	3	9	
Activates Smad & p38	3	5	
Histone acetyltransferase inhibitor	3	3	P1C6
Methyltransferase inhibitors	3	5	
UCH inhibitor	2	3	P1H5
Neurogenesis inducer	2	3	
Adenylate cyclase inhibitors/activates	2	6	
CCR antagonist	2	3	
NF-kB activation inhibitors	2	7	
G-Protein antagonists	2	3	
Related to embryonic stem cells	2	4	
Related to insulin	2	3	
PPARα agonist/antagonists	1	4	
PPARα antagonists	1	2	
Sirtuins activates	1	2	
Histone acetyltransferase activate	1	1	
G-Protein activators/modulators	1	3	

Note: Compounds' full names are in the Supplementary Table S1.
[a]Majority of them are SIRT inhibitors.

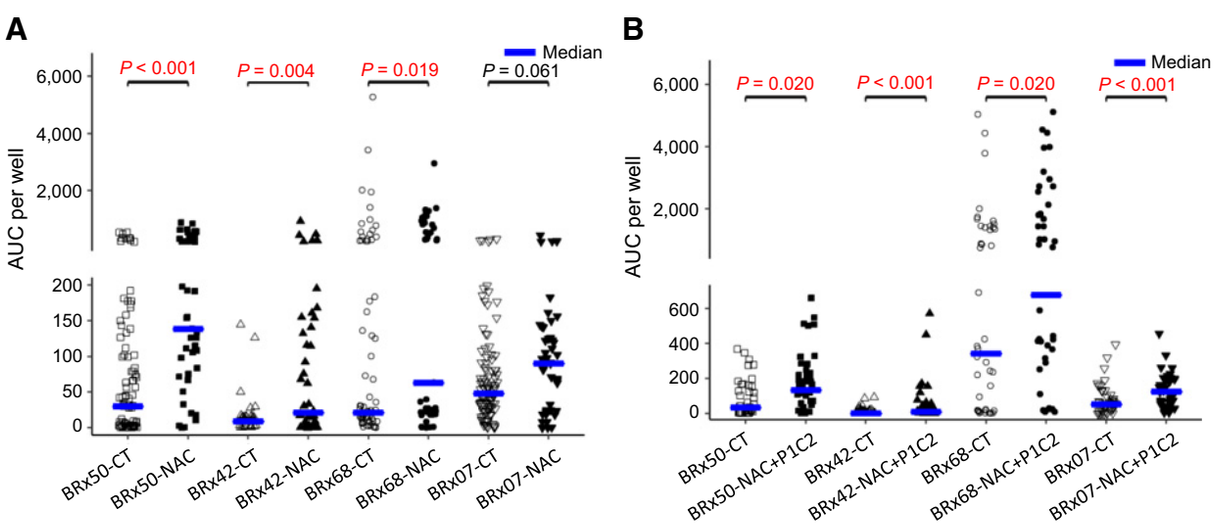

Figure 2.
Compounds promote proliferation of single CTCs. Graph showing AUC measurement of the proliferation of single CTCs from 4 different CTC lines over 24 days with NAC 300 μmol/L (**A**), and NAC + P1C2 (**B**) *P* values were obtained by a Kruskal–Wallis test adjusted by Benjamini–Hochberg procedure for multiple testing.

Published OnlineFirst December 10, 2020; DOI: 10.1158/1541-7786.MCR-20-0482

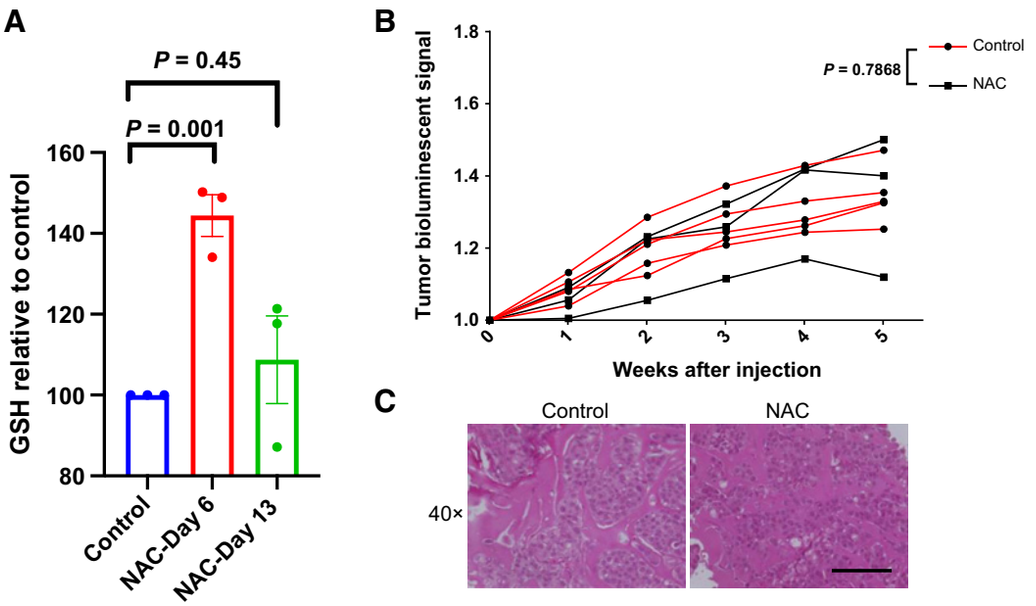

Figure 3.

Pretreatment with short time NAC increased glutathione level but does not change the tumorigenicity of CTCs. **A,** Total glutathione in cells treated with NAC for either 6 or 13 days relative to control untreated cells. **B,** The graph shows the tumor growth kinetics of single BRx68 clones generated with (NAC) or without (control) NAC after the first 24 days (NAC group: $n = 3$, control group $n = 5$). $P = 0.7868$. P value was analyzed by two-way ANOVA with RM by columns between 2 groups at matched time point. Interaction between groups has been tested. **C,** Representative images of hematoxylin and eosin staining of the primary tumor generated in control and NAC groups. Scale bar, 100 μm.

NAC single-cell clones form tumors with similar kinetics as controls

We noticed that the most critical phase is the initial expansion from single CTCs. Once a single-cell colony reaches a critical size, treatment with these compounds (NAC or NAC+P1C2) does not seem to confer additional growth advantages. Indeed, total GSH level in NAC treated cells is significantly higher at day 6, but not at day 13, than that in untreated control cells (44.42 ± 5.165, $P = 0.001$; **Fig. 3A**). Therefore, after 24 days, we stopped the treatment of these compounds and prolonged the culture to generate several single cell clones. To evaluate the tumorigenicity of the single cell clones, we injected GFP-Luciferase tagged BRx68 single clones generated with NAC treatment or control clones into the mammary fat pads of female NSG mice. The NAC treated clones generated tumors with similar growth kinetics and histology, indicating that short term treatment with NAC did not significantly affect CTCs' tumorigenicity (**Fig. 3B** and **C**).

NAC rescued the proliferation of freshly isolated CTCs from a patient with breast cancer

We used our newly developed negative selection method of PIC&RUN assay[25] to isolate live single CTCs from 12 patients with breast cancer and culture them in either NAC containing media or regular media (**Table 2**). In one patient, two single CTCs cultured under regular media divided during the first two weeks; one cell divided once and the other divided twice (**Fig. 4A**). However, shortly after 2 weeks, cells started to die from both clones. In an attempt to rescue these clones, media was replaced with NAC containing media. One clone recovered and resumed proliferation for around 5 more weeks, forming a large colony of cells (**Fig. 4A**). To confirm that these clones are cancer cells, we performed copy number variation (CNV) analyses for 8 single cells isolated from clone 2 after 12 weeks of culture under NAC. CNV profiles of all cells showed global abnormalities resembling that of cancer cells. Moreover, the striking similarity in their global CNV patterns shows that all 8 cells were descended from a single cell (**Fig. 4B**).

Transcriptional analysis of growing and nongrowing single cell clones

To identify the transcriptional changes influenced by these molecules, we performed RNA-seq analysis of pools of growing clones from control or small molecule treated conditions. Principal component analysis (PCA) showed a clear separation of conditions at day 13 versus 6 (**Fig. 5A**), with a dramatic heterogeneity in the control samples at day 13. Differentially expressed genes (DEG) at day 13 versus 6 across all conditions showed enriched genes in lipid metabolism by IPA (Supplementary Table S6). The same lipid metabolism pathway is already enriched at day 6 in NAC and P4D8 (2 antioxidants) treatment compared with control (Supplementary Table S6).

Although NAC treatment significantly induced cell proliferation of single CTCs, many cells were not able to grow even under NAC treatment. This suggests that nongrowing cells in both control and NAC groups may be quiescent, senescent, or a combination of both. Therefore, we conducted RNA-seq for the nongrowing cells from control and NAC. As expected, PCA analysis of the growing versus nongrowing cells showed a clear separation between both groups with high heterogeneity in the nongrowing cells, which is expected as cell proliferation may have masked cell heterogeneity in the growing group (**Fig. 5B**). Heatmap clustering based on senescence and quiescence marker genes identified from a previously published study (20) showed separation between growing and nongrowing cells (**Fig. 5C**; Supplementary Fig. S4A). As expected, the most obvious GO pathway for upregulated DEGs in growing clones at day 13 is cell-cycle regulation

Published OnlineFirst December 10, 2020; DOI: 10.1158/1541-7786.MCR-20-0482

Table 2. Patients clinical information and number of single CTCs cultured under NAC.

Patient ID	Age	ER/PR/HER2	Disease status	Lines of treatments	Site of metastasis	Number of single CTCs cultured under NAC
BC-316	42	$ER^+/PR^+/HER2^-$	SD[a]	1	Visceral	2 out of 12
BC-318	29	$ER^+/PR^+/HER2^+$	PD[b]	5	Visceral + Bone + Brain	4
BC-319	58	$ER^+/PR^+/HER2^-$	SD	1	Bone	20
BC-321	66	$ER^+/PR^-/HER2^+$	PD	4	Visceral + Bone	17
BC-322	59	$ER^-/PR^-/HER2^-$	PD	2	Bone	9
BC-323	48	$ER^+/PR^+/HER2^-$	SD	2	Bone	12
BC-324	53	$ER^+/PR^-/HER2^-$	SD	1	Bone + Breast	40
BC-326	69	$ER^-/PR^-/HER2^+$	SD	5	Visceral	12
BC-327	56	ER^+/PR^+	NA[c]	1	Bone	4
BC-329	48	$ER^+/PR^+/HER2^-$	PD	6	Visceral	31
BC-330	56	$ER^+/PR^+/HER2^+$	SD	4	Visceral	57
BC-331	62	$ER^+/PR^+/HER2^-$	SD	3	Visceral + Bone	12

[a]Stable disease.
[b]Progressive disease.
[c]Not available.

(Supplementary Fig. S4B). By taking the control cells out of the analyses, the clustering between growing and nongrowing NAC-treated clones is even more prominent with senescence markers at day 13 (**Fig. 5D**). Moreover, 6 upregulated DEGs in nongrowing NAC-treated clones overlapped with the 45 senescence markers ($P = 0.079$; Supplementary Table S7). These analyses suggest that nongrowing cells contain a mixture of quiescent and senescent cells and that NAC treatment was able to push a proportion of the quiescent cells into the cell cycle, leaving behind those which are likely enriched for senescent cells.

Discussion

Establishing stable CTC lines is challenging with very low success rates of less than 20% in selected patients with the most aggressive disease stage (7, 10). Many studies have developed novel CTC isolation

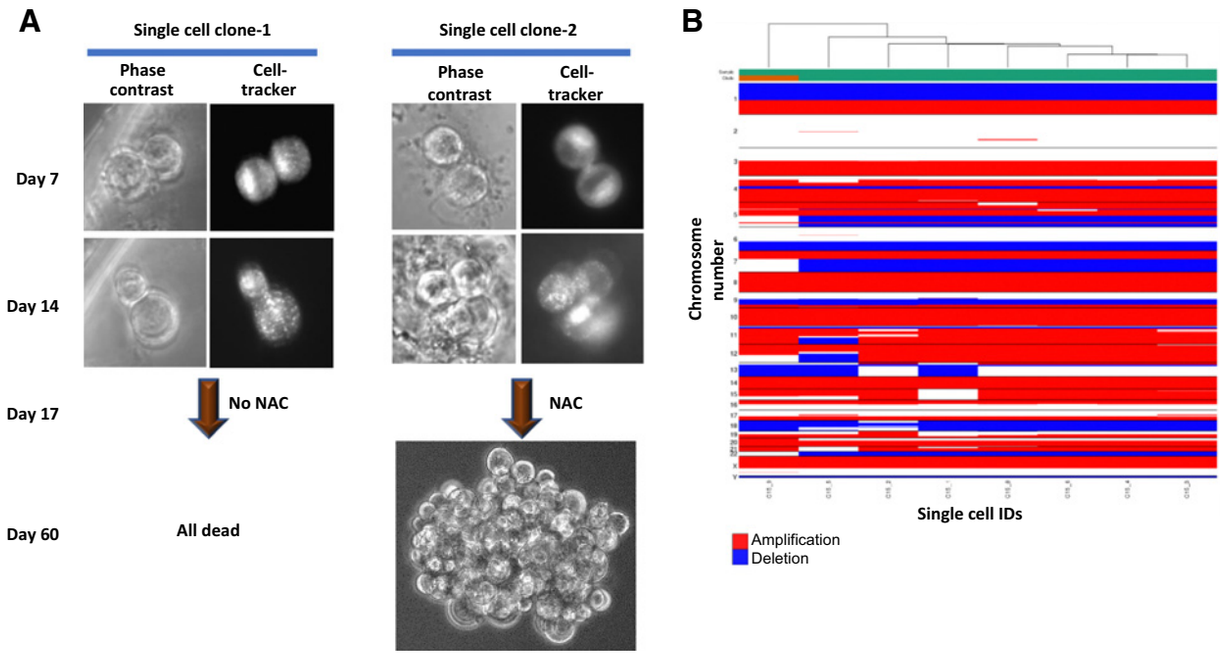

Figure 4.
NAC treatment rescued a CTC clone isolated from a patient with breast cancer. **A,** Two single CTCs were isolated from a tube of blood from a patient with breast cancer were cultured in separate wells. Phase-contrast microscope images and Cell tracker green channel for single-cell clone 1 (left) and 2 (right) at day 7 and day 14 in culture under regular media. Phase-contrast image for single-cell clone 2 at day 60 was shown (after 8 weeks of NAC treatment). **B,** Heatmap showing CNV profiles of 8 single cells isolated from single CTC clone 2 after 12 weeks of NAC treatment.

Published OnlineFirst December 10, 2020; DOI: 10.1158/1541-7786.MCR-20-0482

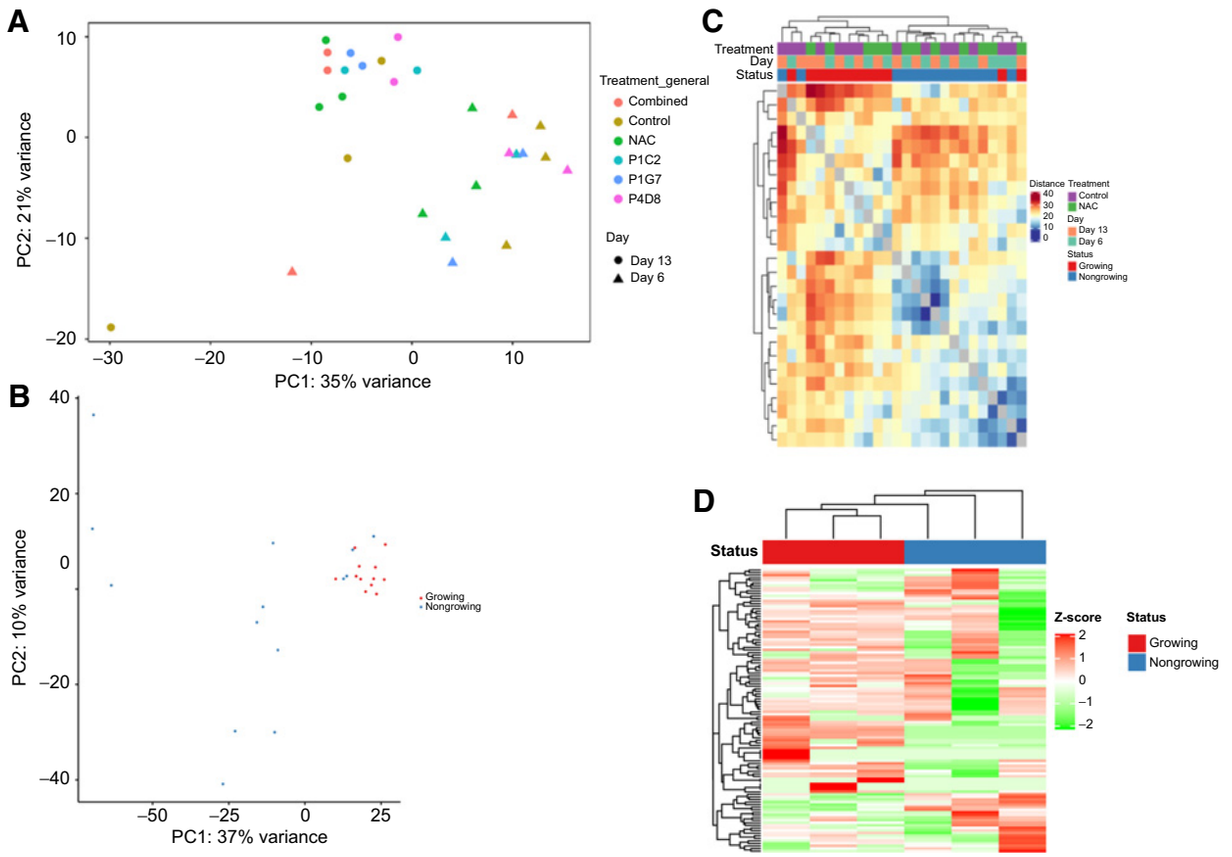

Figure 5.

RNA-seq analysis of growing and nongrowing clones. **A,** PCA plot of RNA-seq results from pools of growing single-cell clones at days 6 and 13 in control- and molecule-treated conditions, including 2 antioxidants (NAC and P4D8) and 2 COX inhibitors (P1C2 and P1G7). **B,** Unsupervised PCA plot for both growing (red) and nongrowing (blue) single-cell clones in control- and NAC-treated conditions. **C,** Heatmap for all samples in **B** based on previously published quiescent and senescent gene signature. Clustering is based on the Euclidean distance between samples. **D,** Heatmap for NAC-treated cells at day 13 based on previously published senescent gene signature. Rows represent *Z*-score of normalized expression values of the marker genes.

methods and tried different culture settings (including hypoxic condition, spheroid, organoid, and 2D culture with the addition of inhibitors to prevent EMT and apoptosis; refs. 10, 26), yet success rates of CTCs *ex vivo* culture is very low and far from being a routine practice. Establishing single CTC clones for functional characterization of CTC heterogeneity is even more challenging. To help overcome this bottleneck, we performed a small molecule library screen on single CTCs from the established breast cancer CTC lines to identify compounds that can promote single CTC expansion *in vitro*. We identified NAC at 300 μmol/L concentration as the best compound for promoting single CTC growth from multiple patient-derived CTC lines and a new breast cancer patient sample. Given the rarity of CTCs isolated from patients, it is impossible to perform such large-scale screening studies directly from freshly isolated CTCs. Although our analysis used already established CTC lines and findings need to be further validated in additional patient samples, this is the first study using patient-derived CTCs to address the critical problem of improving the efficiency in expanding single CTCs *ex vivo*.

Our findings are consistent with the results of recent studies, reporting increased ROS levels in CTCs or cancer cells detached from matrix (23, 24, 27–31). Other studies have demonstrated that this increase in ROS is in fact caused by detachment from the extracellular matrix or loss of cell–cell contact (24, 31). The ROS increase needs to be mitigated via many mechanisms. For example, a fundamental change in citrate metabolism can promote proper redox balance for detached tumor cells (31). Upregulation of free radical scavengers or exogenous antioxidants could also promote the survival of detached tumor cells in circulation (23, 27, 30). In addition to oxidative stress, CTCs must also survive shear stress, immune attack, and physical constriction in the circulatory environment. Furthermore, the isolation procedure, used before *ex vivo* expansion of CTCs, can be a source of stress. Therefore, antioxidant and free-radical scavengers could mitigate these stresses.

During single CTC expansion, RNA-seq analysis showed that NAC induced changes in metabolism, including lipid metabolism, that may promote CTC proliferation. This is consistent with the previous reports on the metabolic changes in tumor cells in suspension (23, 31) and recent demonstration of the importance of lipid metabolism for CTCs (32). The exact role of genes involved in lipid metabolism needs further investigation in the context of single CTC *ex vivo* expansion. Moreover, RNA-seq analysis showed the presence of a heterogeneous population of single cells that are undergoing quiescence or senescence, which presents a challenge for the effort in developing more

Published OnlineFirst December 10, 2020; DOI: 10.1158/1541-7786.MCR-20-0482

efficient ways of culturing CTCs. Our data indicate that NAC may be able to push certain quiescent cells into active cell cycle, an encouraging hypothesis that requires further testing.

We noted that the constraints on proliferation for those CTCs able to grow eventually are significantly reduced once CTCs achieve a critical mass. This suggests that cell–cell contact mitigates stress, in line with recent findings on the survival advantage of CTC clusters (33, 34). This also indicates that compounds promoting CTC proliferation can be applied right after the isolation for a short term and will not confound the downstream characterization of CTC biology, which was supported by data from our xenograft assay using single cell clones from NAC and control groups.

We found that the addition of NAC at 300 μmol/L concentration to CTC culture media was able to promote single CTC proliferation from a new breast cancer patient sample out of 12 tested. This patient had a stable disease after therapy and showed a total of 12 CTCs in 7.5 mL of blood. The majority of CTC stable cell lines previously reported were established from bulk CTCs from patients either off drug or with a progressing disease under treatment and have a very high numbers of CTCs (7–9). Our finding suggests the possibility that NAC may show a higher success rate on bulk CTCs from more patients who are progressing under treatment. However, our sample size is limited due to COVID-19 pandemic, and the broad application of NAC needs further validations with a larger cohort of patients with proper matched comparison in the future.

In summary, through a single-cell screen using breast cancer patient-derived CTC lines, we identified NAC that promotes single CTC proliferation, likely by reducing the stress and altering cell metabolism to facilitate survival and growth. Upon further validation with additional patient samples, this approach potentially can be easily implemented to improve the efficacy of CTC culture.

Authors' Disclosures

I. Kang reports personal fees from Puma Biotechnology, Bristol-Myers Squibb, and Pfizer outside the submitted work. J. Hicks reports grants from Breast Cancer Research Foundation during the conduct of the study as well as personal fees from Epic Sciences, Inc. outside the submitted work. R. Sposto reports grants from US NCI during the conduct of the study. M. Yu reports grants from NIH, Stop Cancer Foundation, PEW Charitable Trusts and the Alexander and Margaret Stewart Trust, the Wright Foundation, and The Richard Merkin Foundation during the conduct of the study, personal fees from Microsensor Labs and other from CanTraCer Biosciences outside the submitted work, as well as a patent 62990445 pending. No disclosures were reported by the other authors.

Authors' Contributions

T. Teng: Resources, data curation, validation, investigation, visualization, methodology, writing–original draft, writing–review and editing. **M. Kamal:** Resources, data curation, formal analysis, validation, investigation, visualization, methodology, writing–review and editing. **O. Iriondo:** Conceptualization, investigation, writing–review and editing. **Y. Amzaleg:** Data curation, formal analysis, visualization, methodology, writing–review and editing. **C. Luo:** Data curation, formal analysis, visualization, methodology, writing–review and editing. **A. Thomas:** Resources, data curation, software, formal analysis, visualization, methodology, writing–review and editing. **G. Lee:** Investigation, writing–review and editing. **C.-J. Hsu:** investigation, methodology, writing–review and editing. **J.D. Nguyen:** Data curation. **I. Kang:** Resources, data curation, writing–review and editing. **J. Hicks:** Resources, formal analysis, supervision, investigation, visualization, methodology, writing–review and editing. **A. Smith:** Resources, software, supervision, writing–review and editing. **R. Sposto:** Data curation, formal analysis, supervision, methodology, writing–review and editing. **M. Yu:** Conceptualization, resources, supervision, funding acquisition, investigation, writing–original draft, project administration, writing–review and editing.

Acknowledgments

We thank the USC Flow Core, USC Histology Core, USC Histology Laboratory and USC Biostatistics Core for their excellent technical support. We thank the USC Department of Animal Resources for the care of our experimental animals. We thank Jeffrey Boyd and Bernadette Masinsin from the USC Flow Cytometry Core for assisting in sorting single cells. We thank Mickey Huang from the USC Choi Family Therapeutic Screening Facility and the Eli and Edythe Broad CIRM Center for Regenerative Medicine and Stem Cell Research at USC for helping to prepare all compounds used in the first round of screening. We are grateful to Cristy Lytal for editing our manuscript. We also thank the following for funding this research: the NIH (DP2 CA206653 to M. Yu), the Stop Cancer Foundation (M. Yu), the PEW Charitable Trusts and the Alexander & Margaret Stewart Trust (M. Yu), the Wright Foundation pilot award (M. Yu), the Richard Merkin Foundation (M. Yu), the Breast Cancer Research Foundation (J. Hicks), and the NIH grant T90DE021982 (trainee Y. Amzaleg). The project described was supported in part (core facilities) by the NCI (grant P30CA014089).

The costs of publication of this article were defrayed in part by the payment of page charges. This article must therefore be hereby marked *advertisement* in accordance with 18 U.S.C. Section 1734 solely to indicate this fact.

Received May 26, 2020; revised September 11, 2020; accepted December 7, 2020; published first December 10, 2020.

References

1. Alix-Panabières C, Pantel K. Circulating tumor cells: liquid biopsy of cancer. Clin Chem 2013;59:110–8.
2. Yu M, Stott S, Toner M, Maheswaran S, Haber DA. Circulating tumor cells: approaches to isolation and characterization. J Cell Biol 2011;192:373–82.
3. Wit S de, Dalum G van, Lenferink ATM, Tibbe AGJ, Hiltermann TJN, Groen HJM, et al. The detection of EpCAM + and EpCAM – circulating tumor cells. Sci Rep 2015;5:12270.
4. Allard WJ, Matera J, Miller MC, Repollet M, Connelly MC, Rao C, et al. Tumor cells circulate in the peripheral blood of all major carcinomas but not in healthy subjects or patients with nonmalignant diseases. Clin Cancer Res 2004;10:6897–904.
5. Kaldjian EP, Ramirez AB, Sun Y, Campton DE, Werbin JL, Varshavskaya P, et al. The RareCyte® platform for next-generation analysis of circulating tumor cells. Cytometry Part A 2018;93:1220–5.
6. Lin E, Rivera-Báez L, Fouladdel S, Yoon HJ, Guthrie S, Wieger J, et al. High-throughput microfluidic labyrinth for the label-free isolation of circulating tumor cells. Cell Syst 2017;5:295–304.e4.
7. Yu M, Bardia A, Aceto N, Bersani F, Madden MW, Donaldson MC, et al. Ex vivo culture of circulating breast tumor cells for individualized testing of drug susceptibility. Science 2014;345:216–20.
8. Cayrefourcq L, Mazard T, Joosse S, Solassol J, Ramos J, Assenat E, et al. Establishment and characterization of a cell line from human circulating colon cancer cells. Cancer Res 2015;75:892–901.
9. Gao D, Vela I, Sboner A, Iaquinta PJ, Karthaus WR, Gopalan A, et al. Organoid cultures derived from patients with advanced prostate cancer. Cell 2014;159:176–87.
10. Maheswaran S, Haber DA. Ex vivo culture of CTCs: an emerging resource to guide cancer therapy. Cancer Res 2015;75:2411–5.
11. Klotz R, Thomas A, Teng T, Han SM, Iriondo O, Li L, et al. Circulating tumor cells exhibit metastatic tropism and reveal brain metastasis drivers. Cancer Discov 2020;10:86–103.
12. Kallergi G, Papadaki MA, Politaki E, Mavroudis D, Georgoulias V, Agelaki S. Epithelial to mesenchymal transition markers expressed in circulating tumour cells of early and metastatic breast cancer patients. Breast Cancer Res 2011;13:R59.
13. Yu M, Bardia A, Wittner BS, Stott SL, Smas ME, Ting DT, et al. Circulating breast tumor cells exhibit dynamic changes in epithelial and mesenchymal composition. Science 2013;339:580–4.
14. Krawczyk N, Meier-Stiegen F, Banys M, Neubauer H, Ruckhaeberle E, Fehm T. Expression of stem cell and epithelial-mesenchymal transition markers in

Published OnlineFirst December 10, 2020; DOI: 10.1158/1541-7786.MCR-20-0482

circulating tumor cells of breast cancer patients. Biomed Res Int 2014;2014: 415721.
15. Papadaki MA, Kallergi G, Zafeiriou Z, Manouras L, Theodoropoulos PA, Mavroudis D, et al. Co-expression of putative stemness and epithelial-to-mesenchymal transition markers on single circulating tumour cells from patients with early and metastatic breast cancer. BMC Cancer 2014;14:651.
16. Polioudaki H, Agelaki S, Chiotaki R, Politaki E, Mavroudis D, Matikas A, et al. Variable expression levels of keratin and vimentin reveal differential EMT status of circulating tumor cells and correlation with clinical characteristics and outcome of patients with metastatic breast cancer. BMC Cancer 2015;15:399.
17. Kamal M, Saremi S, Klotz R, Iriondo O, Amzaleg Y, Chairez Y, et al. PIC&RUN: An integrated assay for the detection and retrieval of single viable circulating tumor cells. Sci Rep 2019;9:17470.
18. Baslan T, Kendall J, Rodgers L, Cox H, Riggs M, Stepansky A, et al. Genome-wide copy number analysis of single cells. Nat Protoc 2012;7:1024–41.
19. Navin N, Kendall J, Troge J, Andrews P, Rodgers L, McIndoo J, et al. Tumour evolution inferred by single-cell sequencing. Nature 2011;472:90–4.
20. Tang H, Geng A, Zhang T, Wang C, Jiang Y, Mao Z. Single senescent cell sequencing reveals heterogeneity in senescent cells induced by telomere erosion. Protein Cell 2019;10:370–5.
21. Gu Z, Eils R, Schlesner M. Complex heatmaps reveal patterns and correlations in multidimensional genomic data. Bioinformatics 2016;32:2847–9.
22. Young MD, Wakefield MJ, Smyth GK, Oshlack A. Gene ontology analysis for RNA-seq: accounting for selection bias. Genome Biol 2010;11:1–12.
23. Piskounova E, Agathocleous M, Murphy MM, Hu Z, Huddlestun SE, Zhao Z, et al. Oxidative stress inhibits distant metastasis by human melanoma cells. Nature 2015;527:186–91.
24. Harris IS, Brugge JS. The enemy of my enemy is my friend. Nature 2015;527: 170–1.
25. Sobolewski C, Cerella C, Dicato M, Ghibelli L, Diederich M. The role of cyclooxygenase-2 in cell proliferation and cell death in human malignancies. Int J Cell Biol 2010;2010:1–21.
26. Wang R, Chu GCY, Mrdenovic S, Annamalai AA, Hendifar AE, Nissen NN, et al. Cultured circulating tumor cells and their derived xenografts for personalized oncology. Asian J Urol 2016;3:240–53.
27. Zheng Y, Miyamoto DT, Wittner BS, Sullivan JP, Aceto N, Jordan NV, et al. Expression of β-globin by cancer cells promotes cell survival during blood-borne dissemination. Nat Commun 2017;8:14344.
28. Schafer ZT, Grassian AR, Song L, Jiang Z, Gerhart-Hines Z, Irie HY, et al. Antioxidant and oncogene rescue of metabolic defects caused by loss of matrix attachment. Nature 2009;461:109–13.
29. Gal KL, Ibrahim MX, Wiel C, Sayin VI, Akula MK, Karlsson C, et al. Antioxidants can increase melanoma metastasis in mice. Sci Transl Med 2015;7:308re8–308re8.
30. Sayin VI, Ibrahim MX, Larsson E, Nilsson JA, Lindahl P, Bergo MO. Antioxidants accelerate lung cancer progression in mice. Sci Transl Med 2014;6: 221ra15–221ra15.
31. Jiang L, Shestov AA, Swain P, Yang C, Parker SJ, Wang QA, et al. Reductive carboxylation supports redox homeostasis during anchorage-independent growth. Nature 2016;532:255–8.
32. Ubellacker JM, Tasdogan A, Ramesh V, Shen B, Mitchell EC, Martin-Sandoval MS, et al. Lymph protects metastasizing melanoma cells from ferroptosis. Nature 2020;585:113–8.
33. Gkountela S, Castro-Giner F, Szczerba BM, Vetter M, Landin J, Scherrer R, et al. Circulating tumor cell clustering shapes DNA methylation to enable metastasis seeding. Cell 2019;176:98–112.e14.
34. Labuschagne CF, Cheung EC, Blagih J, Domart M-C, Vousden KH. Cell clustering promotes a metabolic switch that supports metastatic colonization. Cell Metab 2019;30:720–734.e5.

AACR American Association for Cancer Research

Molecular Cancer Research

N-Acetyl-L-cysteine Promotes *Ex Vivo* Growth and Expansion of Single Circulating Tumor Cells by Mitigating Cellular Stress Responses

Teng Teng, Mohamed Kamal, Oihana Iriondo, et al.

Mol Cancer Res 2021;19:441-450. Published OnlineFirst December 10, 2020.